Forty years of ^{90}Sr in situ migration: importance of soil characterization in modeling transport phenomena

J.M. Fernandez [a,*], E. Piault [a], D. Macouillard [b], C. Juncos [c]

[a] *CEA-Cadarache, DTN/SMTM/LMTE, BP 1, 13108 Saint Paul Lez Durance, France*
[b] *ENSIL, 16 rue d'Atlantis, Technopole BP 6804, 87068 Limoges, France*
[c] *Université de Savoie, BP 1104, 73011 Chambéry, France*

Abstract

In 1960 experiments were carried out on the transfer of ^{90}Sr between soil, grapes and wine. The experiments were conducted in situ on a piece of land limited by two control strips. The ^{90}Sr migration over the last 40 years was studied by performing radiological and physico-chemical characterizations of the soil on eight 70 cm deep cores.

The vertical migration modeling of ^{90}Sr required the definition of a triple layer conceptual model integrating the rainwater infiltration at constant flux as the only external factor of influence. Afterwards the importance of a detailed soil characterization for modeling was discussed and satisfactory simulation of the ^{90}Sr vertical transport was obtained and showed a calculated migration rate of about 1.0 cm year^{-1} in full agreement with the in situ measured values. The discussion was regarding some of the key parameters such as granulometry, organic matter content (in the Van Genuchten parameter determination), Kd and the efficient rainwater infiltration. Besides the experimental data, simplifying assumptions in modeling such as water−soil redistribution calculation and factual discontinuities in conceptual model were examined.
© 2005 Published by Elsevier Ltd.

Keywords: ^{90}Sr; Unsaturated porous medium; Numerical simulation; Experimental plot; Forty years of vertical migration; Data acquisition; Van Genuchten

* Corresponding author. Institut de Recherche pour le Developpement, DME/UR-103, Promenade Laroque, BP A5, 98848 Nouméa, New Calédonia, France. Tel.: +687 26 08 19; fax: +687 26 43 26.
E-mail address: jean-michel.fernandez@noumea.ird.nc (J.M. Fernandez).

1. Introduction

In 1960, the Institute of Nuclear Protection and Safety of the French Atomic Energy Commission (CEA/IPSN) had launched a research program to quantify the soil–plant transfer of ^{90}Sr. The studies were conducted in situ in collaboration with the National Institute for Agronomic Research (INRA) on an experimental site of Mediterranean type (Bovard et al., 1968). These experiments had consisted in contaminating a piece of land prior to planting vines and quantifying the radioactivity transfer from the soil. Since this experiment, the radionuclide has continued to migrate from the surface to the deeper ground layers of the plot under the sole influence of natural atmospheric conditions. The first radiological study since the soil–plant transfer experiments in 1960 (Juncos, 2002) has accurately characterized the plot and the ^{90}Sr distribution as a result of a 40-year period of natural migration throughout the different soil layers.

Although numerous studies have been carried out on the radiostrontium behaviour in soils under controlled laboratory conditions (e.g. Lefèvre et al., 1996; Wang et al., 2003), a reduced number of results have been gained from more close-to-real conditions experiments (e.g. Wiklander, 1964; Forsberg et al., 2000; Forsberg et al., 2001). This work is one of the few field studies on radionuclide migration investigated from real fallout such as Chernobyl accident or former nuclear weapons testing (e.g. Kirchner and Baumgartner, 1992; Arapis et al., 1997) particularly with a migration over such a long period of time (40 years). The large number of analytical data now available, gives, first of all, the opportunity to discuss the relative importance of the phenomena occurring in the transfer of contaminants and allows the ranking of some key parameters of the modeling. It also permits to verify that migration of this radionuclide is being governed by simple phenomena which can be accessed by classic models and to discuss their conditions of applicability as long as some essential data have been acquired.

Simulations were made using the Porflow code (e.g. ACRi, 1994; Ranganathan, 1993; Walton and Otis, 1990) due to its abilities to solve calculations of flows in unsaturated porous media taking into account the sorption/desorption phenomena of chemical species and radioactive decay.

2. Material and methods

The 1960s, experiments had consisted in contaminating a 400 m^2 (10 m × 40 m) piece of land bordered by two uncontaminated strips used as controls (Fig. 1). The plot was labelled by a single sprinkling of 925 kBq m^{-2} of ^{90}Sr in the form of soluble strontium solution (SrCl$_2$). This radioactivity is significant compared with the atmospheric fallouts in the south of France (Galle et al., 2003). The highest values generated by the nuclear weapon tests and the Chernobyl accident being, respectively, 3000 Bq m^{-2} (1966) and 100 Bq m^{-2} (May 7th, 1986).

Prior to planting, the superficial layer of the contaminated plot had been ploughed in order to homogenize the contamination over a depth of about 10 cm.

The modeling of the ^{90}Sr migration phenomena required the acquisition of field parameters to characterize the soil and the contaminant behaviour in situ whenever possible.

2.1. Sampling

Cores 70 cm deep and 8 cm in diameter were extracted, four from the plot area contaminated with ^{90}Sr and four from the control strips. The cores were then sampled into 2 cm thick soil slices and then packed in a polyethylene bag for single use and kept at 4 °C until processing. The samples were then dried in an oven at 40 °C prior to any analytical treatment (granulometry, ^{90}Sr measurements, Kd determination,…).
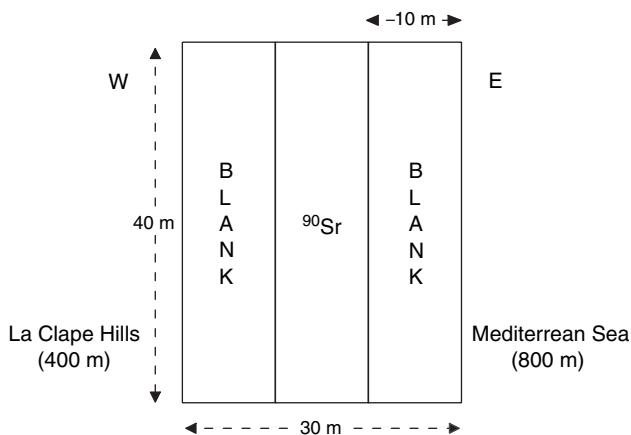
Fig. 1. Diagram of the experimental plot and localization. Boundaries of the ^{90}Sr contaminated strip and both the eastern and western uncontaminated strips.

At the same time, non-handled soil samples were taken in order to measure bulk dry density (ρ_s) and accessible porosity (ω_a) values.

Finally four water table samples were taken in high-density polyethylene bottles (PEHD), and then kept at 4 °C until both the ^{90}Sr and the stable strontium were analysed.

2.2. Granulometry of soil samples

The granulometry influences not only the overall abilities of sorption of a soil (e.g. Ackermann, 1980; Deely and Fergusson, 1994), but also affects the hydraulic characteristics of the latter (e.g. Haverkamp et al., 1998; Romano et al., 1999; Wösten et al., 1999). The granulometric analysis was thus carried out on the sub-samples of each of the four cores so as to obtain access to the Van Genuchten (1980) parameters.

One gram per dry unprocessed soil sub-sample was put into 30 mL of distilled water. The solution was then gently shaken for 1 h and sieved at 200 μm. The bulk fraction was collected, dried and weighed for the calculations. The fine fraction analysis was carried out in triplicate by laser granulometry (Coulter Counter, type LS230), directly on the sieved solution, without adding any dispersal agent or using ultrasonic stirring.

2.3. Geochemical analyses and measurement of ^{90}Sr

The elementary analysis of soils was carried out after acidic digestion by concentrated strong acids (HNO$_3$, HCl, HF) at hot temperatures under hyper baric conditions (Microwave oven Mars-5). The analysis of both the acidic solutions and the ground water was made using ICP-OES (Jobin-Yvon, Ultrace 2000). The composition of the major ions of the ground water was analysed by capillary chromatography (Waters, CIA).

The analysis method of ^{90}Sr was based on the solubilization of the sample followed by a liquid−liquid extraction and finally on the formation of a stable complex which can be measured by liquid β scintillation (Tormos et al., 1995). Briefly, about 10 g of unprocessed sample was calcinated at 550 °C to eliminate the organic matter. The sample was then solubilized in an acidic solution of concentrated nitric acid (65%) and the organic matter destruction was completed by successively adding oxygen peroxide (110 volumes) at hot temperatures. Prior to that, strontium-85 carbonate (^{85}SrCO$_3$) and strontium nitrate (Sr(NO$_3$)$_2$) were added, respectively, as a tracer and a carrier. The strontium was extracted from the acidic solution by an organic phase composed of cyclic polyether at 0.1 M, namely dicyclohexyl-18-crown-6.

The ^{90}Sr present in the ground water samples was directly extracted by the cyclic polyether and then counted.

[90]Sr ($T = 28.6$ year) decays by β^- emission at 546 keV towards the fundamental level of yttrium-90 ($T = 64$ h) which in turn decays by β^- emission at 2284 keV in stable zirconium-90. [90]Sr measurements were carried out using [90]Sr−[90]Y secular equilibrium (10 periods of ^{90}Sr radioactive decay) and [85]Sr to assess the extraction yield.

The detection limit of the β-counter (Wallac, Type Guardian), for a 120 min counting is of 0.1 Bq in the sample. The β measurement results were provided with an uncertainty of 2% on the counting.

2.4. Distribution coefficient (Kd)

[90]Sr mobility in the soil was quantified through its distribution coefficient Kd ($mL\,g^{-1}$), which is defined by ratio between the radionuclide concentration in the solid phase and the concentration in the liquid phase after reaching equilibrium. This constant was experimentally determined and the values of Kds are given by the following overall formula (EPA, 1999a,b):

$$Kd = (C_i - C_r)\frac{V}{C_r m}$$

with C_i = initial tracer concentration, C_r = residual tracer concentration, V = volume of the solution (mL) and m = soil mass (g).

Distribution coefficients were derived from desorption experiments conducted on soil samples with a batch technique modified according to a protocol used by the Radiological Protection and Nuclear Safety (Maubert et al., 1988).

Briefly, in the study 1 kg unsieved soil was sampled from the western control strip of the plot. The distribution coefficients (Kd) were then determined using an experimental contamination technique consisting in saturating with distilled water a manually deposited soil layer of centimetric order and then contaminating it drop by drop with the radioactive solution. This contamination was carried out with 125 mL of solution containing 1 MBq of [85]SrCl$_2$ on several successively deposited layers. The soil thus prepared was stored and maintained wet for a maturing period of one month corresponding to the necessary time required for an acceptable equilibrium to be reached by all the dissolved and particulate phases. The Kd's measurement protocol consisted in sampling 50 ± 0.1 g of saturated soil and extracting the interstitial water with a filtration system under 3 bars of pressure (Millipore membrane, 0.45 μm porosity).

Soil samples were taken from three different layers of soil: the humic layer of the surface (0−5 cm), the sandy clay layer sampled at a depth of 25 cm and the silty clay layer sampled at a depth of 51 cm.

The gamma [85]Sr spectrometry was directly carried out with a Packard Instruments detector (model Cobra II) equipped with a crystal-well NaI of 2 inches at 550 keV.

2.5. Porosity and density

Porosity and density were determined on cylinders of undisturbed soil. The sampling method consisted in pushing the soil into an 8 cm wide and 20 cm long round PVC tube and then pulling it out by digging around it. The tube was then sealed and both ends carefully cut off so as to only keep a soil cylinder of 10 cm in length. The measurement of "accessible porosity" (ω_a) consisted in progressively saturating the soil samples with water until mass stabilization. Water mass gained by the soil cylinder between dry (110 °C, 48 h) and saturated states provided an estimate of the volume of "accessible water" and consequently that of the pores. The bulk dry density (ρ_s) was then deduced from these mass measurements.

2.6. Migration model

The model PORFLOW (Porflow user's manual, 2002) is based on the one hand, on a hydraulic model based on Darcy's law applied to an unsaturated porous medium (Richard's law):

$$\frac{\partial}{\partial t}(\rho\theta\omega) + \nabla(\rho\vec{V}) = m \quad \text{Mass balance equation}$$

$$\vec{V} = -\frac{\overline{\overline{k}}k_r}{\mu}(\vec{\nabla}P + \rho g\,\vec{\nabla}z) = -\overline{\overline{K}}\,\vec{\nabla}h$$

Darcy's law

$$\overline{\overline{K}} = \frac{\overline{\overline{k}}k_r\rho g}{\mu}$$

In these equations ρ = water density; μ = water viscosity; θ = water saturation; ω = porosity of de porous matrix; m = mass injection or withdrawal; V = Darcy velocity; P = pressure; h = hydraulic head; K = hydraulic conductivity tensor; k = reference hydraulic conductivity tensor; k_r = relative permeability and z = elevation.

On the other hand, on a common model of chemical transport which takes into account convective, diffusive and dispersive phenomena, as well as sorption phenomenon.

$$\nabla[\omega D\nabla C + \|\vec{V}\|\overline{\overline{\alpha}}\nabla C - \vec{V}C] = \mathrm{Rd}\omega\theta\left(\frac{\partial C}{\partial t} + \lambda C\right) + S_c \quad \text{Mass transport equation}$$

with D = diffusivity; C = concentration (or activity); α = dispersion tensor; Rd = retardation; λ = decay rate and S_c = source of contaminant.

The model therefore integrates the following parameters:

- The radioactive decay of ^{90}Sr.
- The density and porosity required for each of the three layers of soil in defining the hydraulic behaviour of the unsaturated area (Weng et al., 2001) (Table 2).
- Diffusivity and hydraulic conductivity, the values which are obtained from the bibliography (Brady, 1995; Marimon, 2002) when no experimental values are available (Table 1).
- The retardation coefficient describing the sorption/desorption phenomena, approached using a linear model commonly admitted even though some authors discuss on the non-linearity of ^{90}Sr concentration in soils, especially humic ones (e.g. EPA, 1999a,b; Jinzhou et al., 1996; Xiongxin and Zuyi, 1999). The retardation coefficient (Rd) for unsaturated conditions (Bouwer, 1991), linked to the distribution coefficient (Kd), is given by the following equation:

$$\mathrm{Rd} = 1 + \rho_s \mathrm{Kd}\frac{1 - \omega_a}{\omega_a}$$

with ρ_s = dry bulk density (kg m^{-3}); Kd = distribution coefficient (m^3 kg^{-1}) and ω_a = accessible porosity.

Table 1
Values of hydraulic conductivity and diffusivity used for the simulations

Horizon	Diffusivity (m s^{-2})	Hydraulic conductivity (m s^{-1})
Humus	10^{-8}	10^{-5}
Sandy clay	10^{-9}	10^{-6}
Silty clay	10^{-10}	5×10^{-7}

The hydraulic behaviour of the unsaturated area was approached using retention and analytical conductivity curves (Brooks and Corey, 1966; Mualem, 1972; Van Genuchten, 1980). The selected retention curve (capillary pressure versus water content) consisted in the combination of Van Genuchten's and Mualem's models for the calculation of the relative conductivity and the equation obtained is:

$$K(S) = K_S S^{0.5} \left[1 - \left\{ 1 - S^{1/m} \right\}^m \right]^2$$

$$S = \left[1 + (\alpha \Psi)^n \right]^{-m} \quad \text{if } \Psi > 0$$

$$S = 1 \quad \text{if } \Psi \leq 0$$

and

$$S = \left[\frac{\theta - \theta_r}{\theta_s - \theta_r} \right]$$

with $0 < m < 1$, $m = 1 - 1/n$, $\alpha > 0$, S = saturation, K = hydraulic conductivity (m s^{-1}) and K_s = hydraulic conductivity at saturation (m s^{-1}).

These laws are valid for volume water contents θ ranging from θ_s, the content at saturation to θ_r, the content in residual water.

The governing partial differential equations are solved by the Nodal Point Integration method. The spatial discretization uses the hybrid, the CONDIF or the QUIK numerical scheme. The matrix of algebraic equations resulting from the discretization process is solved by one of the several matrix solutions including NSPCG library (NSPCG user's guide, 1988).

2.6.1. Description of model and boundary conditions

The area studied is represented by a two-dimensional (2D) model due to the isotropy of the soil layers. The movements of ^{90}Sr were only considered on a vertical axis (Y). A vertical 1D model would have been enough to describe the phenomena, however, a 2D model was chosen to be coherent with a future investigation where the influence of the aquifer on the horizontal transport (X) of ^{90}Sr will be studied.

The three layers of the model (Fig. 2) correspond to the layers actually involved in the migratory phenomena of ^{90}Sr, the layer of grey compact clays not being represented because of its very low permeability. The considered soil system is: 70 cm deep, 1 m thick and 200 cm wide.

The vertical migration of ^{90}Sr being mostly influenced by the infiltration of rainwater, the boundary conditions are as follows.
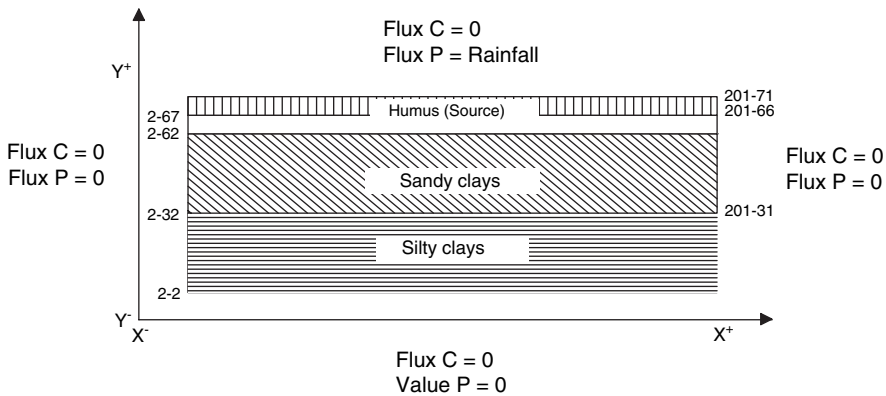

Fig. 2. Diagram of the model corresponding and boundary conditions.

2.6.1.1. Concentration conditions

- On the X^- and X^+ boundaries the model is considered as infinite, which means considering the symmetry conditions in X^- and X^+.
- In Y^+, no flux is assumed since the source is contained in a soil layer 10 cm thick (hypothesis of study). In Y^-, the presence of the grey clay layer as a watertight barrier does not allow exchanges of matter.

2.6.1.2. Water head conditions

- In X^+ and X^-, no pressure flux is observed for the same conditions as above.
- In Y^+, a flux entering the system (therefore positive) is imposed. It corresponds to a yearly average of efficient atmospheric precipitations evenly distributed over all the surface of the study. In Y^-, a zero pressure value is imposed, which is characteristic of a low boundary of the model completely permeable to water (fictional water table level). This condition is necessary in this case as the head of the water table is not taken into account.

The model as defined above is discretized into quadrangles. The grid includes 202 elements along the X-axis and 72 elements along the Y-axis. The surface of the grid elements is of 1 cm^2. The values of the fields are assumed to be constant within each grid element.

2.6.2. Conversion of results from simulations

The calculation code provided radioactivity values in Bq m^{-3} of water, whereas the content in ^{90}Sr measured in the soil samples is expressed in Bq kg^{-1}, unit from the β counting; therefore a conversion is necessary to first work on concentrations expressed in Bq m^{-3} of total soil (soil + interstitial water) then in Bq kg^{-1} of dry soil.

The estimation of the radioactivity present in the total soil can be calculated by considering 1 m^3 of matter. The volumes of the two phases making up the environment are:

$$V_s = 1 - \omega_a$$
$$V_w = \omega_a S$$

with ω_a = accessible porosity and S = saturation.

In an unsaturated medium, the Kd is given by the formula:

$$Kd = \frac{C_s}{C_w S}$$

with C_s = concentration of ^{90}Sr contained in the solid fraction (Bq kg^{-1}) and C_w = concentration of ^{90}Sr contained in the aqueous fraction (Bq m^{-3}).

For each phase, the radioactivity expressed in Bq in 1 m^3 of soil is:

$Q_s = C_s (1 - \omega_a)\rho_s$, in the soil fraction;
$Q_w = C_w \omega_a S$ in the interstitial water;

with ρ_s = bulk dry soil density (kg m^{-3}).

The total concentration C_T in ^{90}Sr (soil + interstitial water) in Bq kg^{-1} is thus:

$$C_T = \frac{(Q_s + Q_w)}{M_s} = \frac{C_s S[Kd(1 - \omega_a)\rho_s + \omega_a]}{(1 - \omega_a)\rho_s}$$

with M_s = mass of the soil fraction.

3. Results and discussion

3.1. Characterization

3.1.1. Climatologic, aquifer and pedology

The experimental site is submitted to a typically Mediterranean climate, characterized by very abundant rains in the fall. A Meteo-France's weather station located nearby allowed the determination of the annual rainfall which has an average of 587.5 mm rain over the last 35 years.

However, only a fraction of the rainwater quantity yearly measured penetrates into the soil because of the intense evapo-transpiration mechanisms described for this Mediterranean area. In the absence of accurate studies conducted in situ, the ''efficient infiltration'' in this soil can be considered at about 65% of yearly rainfall, in other terms 381.9 mm year^{-1} (1.21 × 10^{-8} m^3 s^{-1}, estimated data from INRA). This value can be acceptable considering that only rainfalls over 2 mm seem to be able to refill the aquifer because of the existing foliage (Juncos, 2002). The magnitude of the refill directly fluctuates with the intensity and occurrence of the local rainfall. Besides, the electrical conductivity records show that the intrusion of briny water, due to the presence of coastal marshes, is regularly detected depending on the local weather conditions: fall eastern winds (Juncos, 2002).

The pedological study showed that the soil in the plot was composed of a topsoil of more or less silty−sandy clays in the first 70 cm and compact grey clays remarkably poor in water content at the bottom. More precisely, this soil consists of four layers, individually isotrope, on the scale of the experimental plot (Table 2):

- *A humic surface layer*: Since the last 1963 experiments, foliage progressively covered the plot generating the formation of a humus layer of about 5 cm thick.
- *A sandy clay layer surmounting a silty clay layer*: These correspond to two successive deposits of alluvial particles. These layers together represent an average soil thickness of 65 cm.
- *A compact grey clay layer*: Very poor in water content ($\theta < 15−20\%$), this layer is relatively rich in reduced organic matter inherited from the pre-existing coastal marshes. This layer is an efficient tight barrier for the temporary aquifer.

3.1.2. Profile of ^{90}Sr radioactivity in the soil

The analysis of the centimetric samples taken from the four cores helped to plot the average model profile of ^{90}Sr radioactivity over all the thickness of the topsoil (Juncos, 2002). The main observations are (Fig. 3):

- A radioactivity peak (157 Bq kg^{-1}) measured in the humus layer (0−5 cm).

Table 2
Diagram description of horizons making up the stratigraphic series of the experimental plot soil

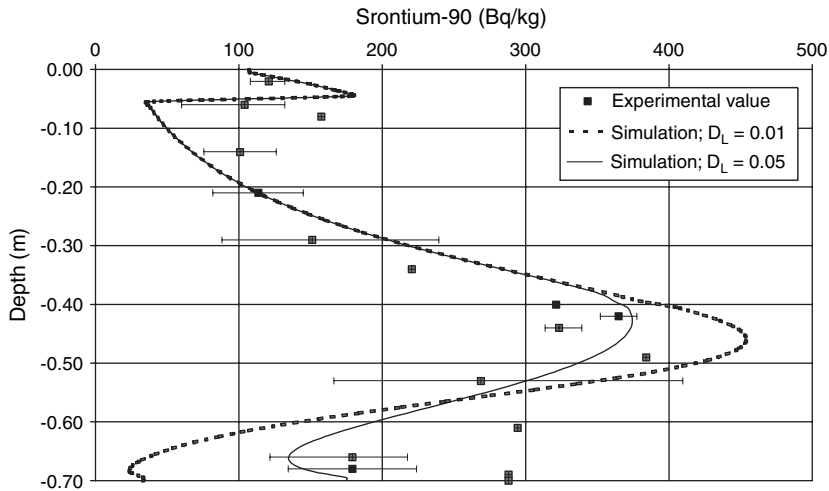| Depth (cm)	Log	Clays (% < 2 μm)	Silts (2 < % <50 μm)	Sands (% > 50 μm)	Density (g L^{-1})	Porosity (%)
0−5	Humus + fine sand	5.0	24.6	70.4	1200	0.60
5−40	Sandy clays	8.1	26.5	65.4	2210	0.37
40−70	Silty clays	12.5	46.7	40.8	2140	0.36
70−83	Compact grey clays	33	52	15	−	−

Fig. 3. Average profile ($n = 4$) of ^{90}Sr radioactivity in the contaminated soil strip. Comparison of experimental results and migration simulation of ^{90}Sr over 40 years. A longitudinal dispersion (D_L) of 0.05 m^2 s^{-1} (dark curve) enhances the simulation of the ^{90}Sr accumulation at the bottom of the silty clay layer with nearly permanent saturated conditions.

- A main migration front, of about 370 Bq kg^{-1}, located at a depth between -45 and -50 cm corresponding to a measured migration rate of about $1.1-1.2$ cm year^{-1}.
- An accumulation of ^{90}Sr visible at the interface between the watertight layer made of grey clays ($h = -70$ cm) and the silty clays.

The surface radioactivity (Bq m^{-2}) of this model profile was calculated by integrating the measured radioactivity, the sampled mass, and the average values of the dry density and porosity. The calculation shows that the fixed radioactivity is about 298.5 kBq m^{-2} of ^{90}Sr and that this amount represents roughly 90.3% of the theoretical residual radioactivity (330.5 kBq m^{-2}). This proportion matches the assessment obtained by Juncos (2002), who demonstrated the present contamination of the control strip highlighting the lateral exportation of ^{90}Sr towards the downstream part of the plot. This export represented $10-14\%$ of the initial injected radioactivity.

3.1.3. Distribution coefficient

The tests conducted in the laboratory on soil samples, showed that the values of the distribution coefficients of ^{85}Sr of the two deepest layers were relatively equivalent: 46 ± 4 mL g^{-1} in the $22-24$ cm layer and 41 ± 13 mL g^{-1} in the $52-54$ cm layer. A greater order of magnitude was obtained for the humus layer (0–3 cm): 249 ± 60 mL g^{-1}.

Directly linked to the clay content, the cationic exchange capacity (CEC) seems to be the main parameter governing the strontium Kd (Lefèvre et al., 1993) making the reaction potentially reversible (Serne and Le Gore, 1996). However, some studies mention a non-negligible fraction ($10-50\%$) which is difficult to remobilize (Brady et al., 1998). This behaviour was specifically described for acidic soils where strontium would substitute to calcium as already mentioned by Wiklander (1964) and Taylor (1968). These previous results could explain the relatively high value of the Kd measured in the humus layer of the topsoil where the calcium concentration reaches roughly 10% of the mass (Juncos, 2002).

Table 3
Stable Sr concentration and measurement of ^{90}Sr radioactivity in the water and soil samples

	Depth (cm)	Water	Soil	Kd (mL/g)
^{90}Sr	54–60	0.048 Bq mL^{-1}	0.26 Bq g^{-1}	5.4
	60–65	0.020 Bq mL^{-1}	0.05 Bq g^{-1}	2.5
Sr stable	54–60	6.0 μg g^{-1}	236.0 μg g^{-1}	39
	60–65	9.3 μg g^{-1}	418.5 μg g^{-1}	45

For the two deepest layers, the values of the distribution coefficient determined experimentally are remarkably similar to those of the average Kd assessed by analysing both the stable strontium in the soil and the ground water samples (Table 3). These similarities can be partly explained by experimental contact times long enough to simulate the natural conditions found in situ. In this case, the measured concentrations are probably regulated by the ''dissolution/co-precipitation'' of strontium associated to calcite and anhydrite (Faure and Powell, 1972) and to a lesser degree to the equilibrium with strontianite, potentially present at these pHs, in slight under-saturation in the experimental soil (Juncos, 2002).

The Kds calculated by the ^{90}Sr measurements in the samples showed very low values (Table 3). These assessments were obtained from samples taken during an incursion of briny waters ([Na] > 2000 mg L^{-1}), which made the water table swell by about 20 cm. In this context, the effect of the ionic strength is added to the ionic competition with the dissolved calcium ([Ca] > 1000 mg L^{-1}). Together, these two conditions can explain the low Kd values which will partly assist the reversibility of the adsorption reaction of the radionuclide when the ^{90}Sr is initially introduced in salt form (EPA, 1999b).

These ''marine'' episodes have an occurrence, amplitude and duration low enough (Juncos, 2002) to ignore the corresponding Kd values. The Kd values used in the simulation were those obtained from the laboratory study.

3.1.4. Granulometry and Van Genuchten parameters

The Van Genuchten model needs the determination of parameters n (porosity size distribution index), α, θ_r (residual water content) for the calculation of ''suction versus saturation'' functions. The three values are greatly dependent on the texture and composition of the soil, the fourth parameter, θ_g (residual content of the gaseous phase) will not be considered in this study.

No value for n and α can be obtained by direct measurements on the experimental soil and even residual saturation ($S_{res} = \theta_r/\omega$) determination is not really easy to get routinely. Therefore their determination had to be approached through databases (Table 4). This type of approximation required the detailed study of the different grain size populations of clays ($d < 2$ μm), silts (2 μm $< d < 50$ μm) and sands ($d > 50$ μm). The granulometric distribution then allowed to look in the databases for the soils with similar characteristics [Grizzly (Haverkamp et al., 1998), ERP (Khaleel and Freeman, 1995; Romano et al., 1999) or HYPRES (Wösten et al., 1999) or still UNSODA (Simunek et al., 1996)] even though for the latter the access to the n and α parameters is not direct.

In terms of granulometric composition, several soils suggested by the different databases match with the three layers determined from the experimental plot. However, for each layer the values attributed to n and α significantly vary from one referenced sample to another. This difference is even greater between two databases such as Grizzly and ERP (Table 4). Fig. 4 shows two theoretical soil kinetics of water retention presenting similar granulometric

Table 4
Composition of experimental plot horizons and correspondence with soil types (Grizly and ERP)

	Soil	MO (%)	Clays (%)	Silts (%)	Sands (%)	Van Genuchten parameters	
						α (m^{-1})	n
Plot	Humus	≈ 4.0	4.9	24.7	70.4		
Grizzly	G-141	0.1	4.77	26.84	68.40	2.2949	2.191
	G-138	1.8	4.90	26.67	68.42	3.9014	2.265
	G-132	3.4	5.19	21.41	73.40	2.4240	2.339
	G-149	6.4	5.05	20.94	74.01	3.2180	2.308
	G-155	4.7	5.36	20.85	73.78	9.0430	2.261
Plot	Clays + sands	2.3	8.1	26.5	65.4		
Grizzly	G-151	0.3	7.81	24.57	67.62	7.9101	2.241
	G-119	1.7	7.93	22.92	69.14	11.5104	2.184
	G-221	1.7	7.96	25.48	66.56	6.3403	2.361
	G-706	0.2	8.15	24.77	67.08	5.8872	2.242
ERP	VOC 3-0655	–	6	24	70	3.4483	1.6285
	241-T-106_3-0688	–	6	28	66	2.7777	1.6568
	241-T-106_3-0689	–	9	25	66	4.5454	1.6651
Plot	Clays + silts	3.3	12.5	46.7	40.8		
Grizzly	G-672	1.9	12.17	46.69	41.13	1.5469	2.200
	G-701	1.6	12.50	46.80	40.70	3.1671	2.209
	G-584	1.6	12.56	41.90	45.54	1.4586	2.175
	G-293	1.2	12.71	40.23	47.06	0.2374	2.279

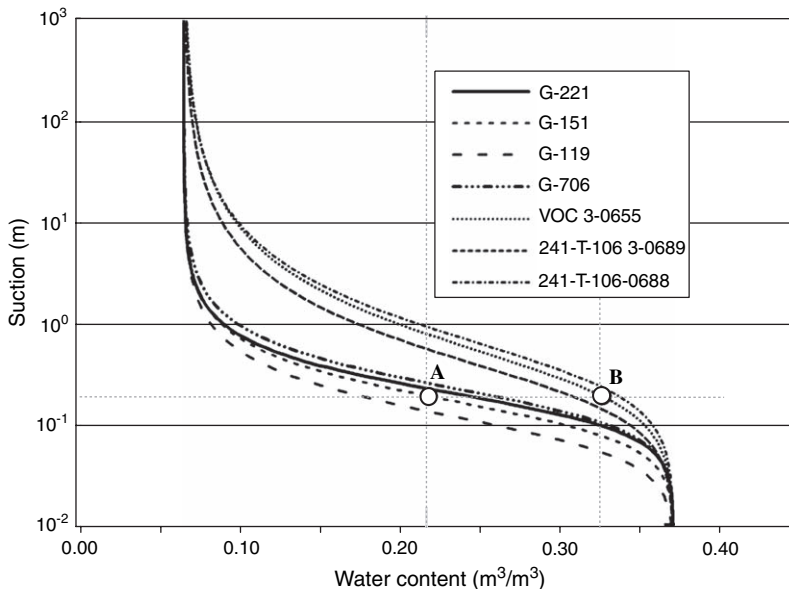Van Genuchten–Mualem model parameters for typical soils.

Fig. 4. Suction versus water content curves established using Van Genuchten (n and α) parameters provided by the Grizzly and ERP databases for soils presenting similar granulometric characteristics. Water content at a suction of 0.185 m for referenced Grizzly soils (A; 50%) and ERP soils (B; 15%), n values are, respectively, 2.26 and 1.65.

compositions: 50% of the water content is reached at a suction of 0.185 m for the referenced Grizzly soils (A), and only 15% for the referenced ERP soils (B) characterized, respectively, by n values of about 2.26 and 1.65. These values showing different hydraulic behaviours are probably due to the relative advanced level of organization of particles in the referenced sedimentary structures mentioned in the databases. The water retention curves from the ERP database soils could then mirror the effects of compaction in the relatively deep sampled sedimentary layers (-36.9 to -52.2 m) of the core, a phenomenon which hardly exists in the sub-surface sample soils (0 to -0.7 m) of the studied experimental plot.

Consequently, the hydraulic behaviour of the layers of the experimental plot seems to be best described by the referenced sub-surface soils of the Grizzly database. However, the selection of value couples in the latter is dependent on a new parameter: the content in organic matter (OM) which determines between soils with similar granulometric compositions.

For each of the three layers of the experimental plot, the Grizzly database thus proposes soils whose characteristics have satisfactory similarities with the experimental values obtained in this study. The referenced soils selected were, therefore, G-132 for the humus layer, G-221 for the sandy clay layer and G-701 for the silty clay layer (Table 4).

3.2. Modeling

3.2.1. Source term

Since the code takes into account the aqueous phase for the calculations, the ^{90}Sr radioactivity must be expressed in Bq m^{-3} of water. For the source term the latter must be calculated in the first 10 cm of the topsoil (Fig. 2); 50% of which is located in the humus layer (5 cm) and 50% in the sandy clay layer (5 cm), by hypothesis.

A theoretical saturation profile (Fig. 5) was calculated from a simulation based on both the assumptions of steady-state flow and the three-soil-layers conceptual model. This calculation provided the average saturation rates for the two layers making up the source term as described. The values are, respectively, 0.7711 and 0.4789.
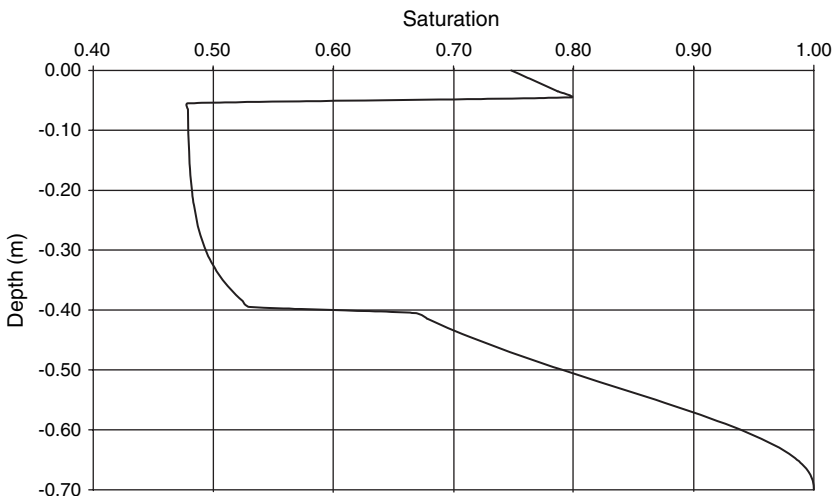

Fig. 5. Water saturation versus depth in the experimental. Profile simulated in steady-state flow.

The contamination value per fluid volume unit (Bq m^{-3}) requires the volume of water to be determined in the two topsoil layers containing the source, according to the following expression:

$$V_{\text{water}} = \text{area volume} \times \text{saturation} \times \text{porosity}$$

The total volume of water (0.0640 m^3) is thus distributed according to:

$$V_{\text{water in humus}} = [0.05 \times 1 \times 2] \times 0.7711 \times 0.60 = 0.0463 \text{ m}^3$$

$$V_{\text{water in sandy clays}} = [0.05 \times 1 \times 2] \times 0.4789 \times 0.37 = 0.0177 \text{ m}^3$$

The present modeling step excludes the lateral transport by the aquifer, therefore only about 90% of this initial radioactivity must be taken into account which matches the previous assessments by Juncos (2002). The radioactivity making up the source term is thus of 1,670,896 Bq for the 2 m^2 section model containing 0.0640 m^3 of water. The total theoretical radioactivity of the aqueous phase is equal to 26,108,367 Bq m^{-3}.

The retardation factor (Rd) being equal to 234.3 for the humus layer and 208.0 for the sandy clay layer, the radioactivity for both layers of the source term is therefore of 236,959 distributed as:

Humus source: 26,108,367/234.3 = 111,415 Bq m^{-3} of water.
Clay source: 26,108,367/208.0 = 125,543 Bq m^{-3} of water.

3.2.2. Migration simulation

The theoretical saturation profile (Fig. 5) shows that the three superimposed soil layers react individually to the water flowing through the domain. Moreover, the results underline relatively high values of saturation due to the rainwater flux in conjunction with the parameters' values describing the different layers and the reduced dimensions of the sedimentary structure. The conditions imposed lead to the appearance of a beginning of saturation in the lower part of the domain.
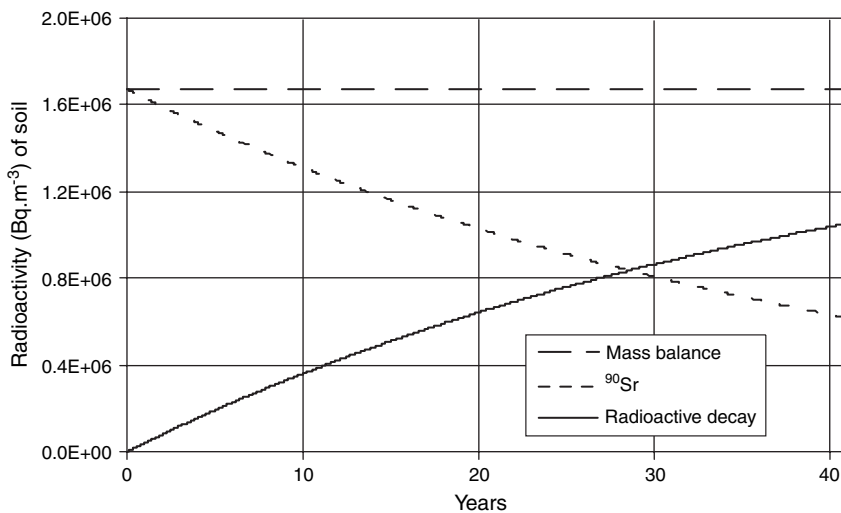

Fig. 6. Mass balance over a 40 years simulation of ^{90}Sr migration in the soil.

Fig. 6 shows that the mass balance is correct and that the most part of ^{90}Sr is lost by radioactive decay at 40 years.

Curves resulting from two numerical simulations and the analytical values of the experimental data are shown in Fig. 3. The measured values come with error bars representative of the analytical dispersion when several samples were measured.

These simulated profiles result in the following remarks:

- A good coherence is observed between the simulation and the experimental data (dots), the calculated migration rate (1.0 cm year^{-1}) being in full agreement with those obtained in Mediterranean calcic luvisol (Forsberg et al., 2000). However, in terms of quantification, the calculated values overestimate the radioactivity of the migration front and inversely, do not account for the phenomenon of radionuclide accumulation in contact with the watertight floor made up by the grey clay.
- A much better simulation underlying the accumulation of ^{90}Sr at the bottom of the silty clay layer is obtained by increasing its longitudinal dispersion (D_L) value from 0.01 to 0.05 m^2 s^{-1}. The latter is within the acceptable limits discussed by Gelhar (1993) when assumed the last 20 cm of the silty clay layer are influenced by the nearly permanent presence of a reduced aquifer (Fig. 3).
- At the "humus−sandy clay" interface, the difference between the simulations and the measurements is obvious. This underlines the drastic discontinuity pre-defined with characteristics proper to the two layers of the model.
- An overall acceptable quantification of Kd even though minor adjustments were applied to the experimental results of the deepest two layers. The values which coincide with the best adjustment of the model are gathered in Table 5.

Table 5
Summary of main parameters characterizing the three modeled horizons

		Humus	Sandy clays	Silty clays
Experimental parameters	Kd (m^3 kg^{-1})	0.25	0.05	0.04
	ρ_s (kg m^{-3})	1400	2210	2140
	ω_a	0.60	0.37	0.36
Van Genuchten parameters	n	2.339	2.361	2.209
	α	2.4242	6.340	3.167
	Sr	0.0391	0.0627	0.0628
	Sg	0	0	0
Hydraulic conductivity	K_x, K_y (m s^{-1})	1×10^{-5}	1×10^{-6}	5×10^{-7}
Diffusivity	D_M (m^2 s^{-1})	10^{-8}	10^{-9}	10^{-10}
Dispersion	D_T (m^2 s^{-1})	0	0	0
	D_L (m^2 s^{-1})	0.010	0.010	0.05
Organic matter	MO (%)	≈ 4.00	2.33	3.25
Rainfall	(mm an^{-1})		587.5	
Efficient rainfall	(mm an^{-1})		381.9 (=65%)	
Initial source term	(kBq m^{-2})		925	
Simul. source term	(kBq m^{-2})		835.5 (=90.3%)	

Theses discrepancies can partly be attributed to the conceptual aspects of the model due to the simplification of the media and the uncertainties related to the experimental techniques or when parameter values were acquired from the bibliography.

3.2.2.1. Technical and/or analytical factors. For the needs of numerical simulation, the mobility of ^{90}Sr in the environment is described using several empiric parameters (n, α and θ_r), which often have to be extracted from databases of soil characteristics. Prior to the acquisition of these parameters, granulometric composition and organic matter content require accurate determination and even though these are elementary, they lead to the classification of soil versus clay, silt and sand proportions. Consequently, this classification results in selecting Van Genuchten parameters to best describe the hydraulic behaviour of soil layers.

Among the decisive experimental parameters used when simulating, the distribution coefficient (Kd) needs to be accurately determined for each layer of the conceptual model and its value must be as realistic as possible.

For other measured parameters, e.g. atmospheric precipitations, the calculations based on an average yearly value instead of a monthly value, do not seem to greatly affect the simulation results. However, although the evaluation of the water infiltration rate for a given soil turns out to be logically of uppermost importance for the simulation, this value is actually difficult to reach in most cases. Thus, there is a variation of 10% of the entering rain flux which significantly changes the migration profile of the ^{90}Sr in the experimental plot soil. The latter was estimated using data from a similar Mediterranean soil now studied by the INRA where in situ measurements of evapo-transpiration values were carried out.

Despite a relatively good soil homogeneity, an accurate sampling technique of any interface (e.g. humus–sandy clays) could greatly reduce the standard deviation of the analytical data.

3.2.2.2. Conceptual factors. The simulation of the ^{90}Sr migration through unsaturated porous media needs previous calculation steps in steady-state flow. Apart from this simplifying assumption, no set of experimental values was available for the water redistribution validation in soil.

The description of the model requires the discretization of the study media and the superimposition of three domains (layers) with very different characteristics. When calculating from a layer to the next these respective parameter values are used without transition. This is the case for the humus–sandy clay interface, which is probably formed by a more or less thick mixing zone where the retardation factor (Rd) of ^{90}Sr progressively decreases from the humus towards the sandy clay.

The longitudinal dispersion (D_L) is one of the non-experimental parameters enumerated to be assessed in a sensitivity analysis. Better simulations could be achieved by choosing variable D_L values to each medium as a function of the water table level.

These factual discontinuities in the conceptual model underline the limits of the modeling which have already been shown by the need to extract from bibliographic approximation of some parameters (n, α, S_r, D_M,...) for assumed similar soils.

4. Conclusion

The modeling of the vertical migration of ^{90}Sr through the soil of the experimental plot required the definition of a triple layer conceptual model which was abundantly characterized and whose only external factor of influence taken into account was the rainwater at constant flux.

Due to the importance of the representativity of the data sets when modeling, the parametering must be based, as much as possible, on values ensured by the in situ collection or must be the result from laboratory analyses. However, since a complete experimental characterization is not possible in most cases, it appears that there must be a ranking in data acquisition and in the integration of the phenomena.

For instance, the characterization of the site allowed the event phenomena to be decoupled distinguishing from the infiltration of the rainwater, as the mainspring of the vertical migration, the other two secondary factors responsible of the lateral transport of ^{90}Sr (Juncos, 2002). These two latter phenomena were therefore identified and can be related with the regime of atmospheric precipitations which varies greatly depending on the season in the Mediterranean climate. The resulting significant piezometric fluctuations should have a great incidence on the dispersion coefficients of the radionuclide.

Besides data directly governing the migration kinetics (Kd, Rd), grain size distribution needs to be accurately performed as the basis for the Van Genuchten parameters selection through soil databases. The choice between databases is crucial in the selection of the parameter values and must depend on both the organic matter content availability and the granulometric population statements. The latter substantially differs between two databases in the clays and silts cutting size definitions what consequently changes the mass percentages of the grain-sized populations and then the n and α corresponding values.

Some key parameters, other than the linearity assumptions of the ^{90}Sr sorption phenomenon for a carbonate soil, are hence subject to be discussed; this is the case of the assessment of the actual water infiltration flux which greatly differs from one site to another and thus greatly influences the calculations of ^{90}Sr migration rates. Therefore around the Mediterranean Sea, wind must be considered as a main climatic factor influencing the evapo-transpiration balance, accordingly the infiltration rainwater rate into the soil.

Acknowledgement

References

Ackermann, F.A., 1980. Procedure for correcting the grain size effect in heavy metal analyses of estuarine and coastal sediments. Environmental Technology Letters 1, 518−527.

ACRi, 1994. PORFLOW: A Software Tool for Multiphase Fluid Flow, Heat and Mass Transport in Fractured Porous Media − Validation. Version 2.50. Analytic & Computational Research, Inc., Los Angeles, Utica, CA.

Arapis, G., Petra yev, E., Shagalova, E., Zhukova, O., Sokolik, G., Ivanova, T., 1997. Effective migration velocity of ^{137}Cs and ^{90}Sr as a function of the type of soils in Belarus. Journal of Environmental Radioactivity 34, 171−185.

Bovard, P., Delmas, J., Grauby, A.P., Benard, P., 1968. Transfert des produits de fission dans la vigne et le vin. Académie d'agriculture de France, extrait du procès-verbal de la séance du 23 octobre 1968, pp. 989−995.

Bouwer, J., 1991. Simple derivation of the retardation equation and application to preferential flow and macrodispersion. Ground Water 29 (1), 41−46.

Brady, J.B., 1995. Diffusion data for silicates minerals, glasses and liquids. In: Ahrens, T.H. (Ed.), Mineral Physics and Crystallography: A Handbook of Physical Constants, AGU Reference Shelf2. American Geophysical Union, Washington, D.C., pp. 269−290.

Brady, P.V., Cygan, R.T., Nagy, K.L., 1998. Surface charge and metal sorption to Kaolinite. In: Jenne, E.A. (Ed.), Adsorption of Metals by Geomedia. Variables, Mechanisms, and Model Applications. Academic Press, San Diego, California, pp. 371−382.

Brooks, R.H., Corey, A.T., 1966. Properties of porous media affecting fluid flow. Journal of the Irrigation and Drainage Division, Proceedings of the American Society of Civil Engineers 92 (IR2), 61−87.

Deely, J.M., Fergusson, J.E., 1994. Heavy metal and organic matter concentrations and distribution in dated sediments of a small estuary adjacent to a small urban area. The Science of the Total Environment 153, 97−111.

Environmental Protection Agency, 1999a. Understanding variation in partition coefficient, Kd, values. In: The Kd Model, Methods of Measurement and Application of Chemical Reaction Codes, vol. 1. 402-R-99-004A.

Environmental Protection Agency, 1999b. Understanding variation in partition coefficient, Kd, values. In: Review of Geochemistry and Available Kd Values for Cadmium, Caesium, Chromium, Lead, Plutonium, Radon, Strontium, Thorium, Tritium, and Uranium, vol. 2. 402-R-99-004B.

Faure, G., Powell, J.L., 1972. Strontium Isotope Geology. Springer-Verlag, Berlin, Germany.

Forsberg, S., Rosén, K., Fernandez, V., Juhan, H., 2000. Migration of ^{137}Cs and ^{90}Sr in undisturbed soil profiles under controlled and close-to-real conditions. Journal of Environmental Radioactivity 50, 235−252.

Forsberg, S., Rosén, K., Bréchignac, F., 2001. Chemical availability of ^{137}Cs and ^{90}Sr in undisturbed lysimeter soils maintained under controlled and close-to-real conditions, 50, pp. 235−252.

Galle, P., Paulin, R., Coursaget, J., 2003. Données métrologiques et évaluation des risques en France lors de l'accident de Tchernnobyl (26 avril 1986). Mise au point historique. Comptes Rendus Biologies 326, 699−715.

Gelhar, L.W., 1993. Stochastic Subsurface Hydrology. Prentice Hall, New York.

Haverkamp, R., Zammit, C., Bouraoui, F., 1998. Grizzly Soil Data Base. http://www.lthe.hmg.inpg.fr/Grizzly/.

Jinzhou, D., Wenming, D., Xiangke, W., Zuyi, T., 1996. Sorption and desorption of radiostrontium on calcareous soil and its solid components. Journal of Radioanalytical and Nuclear Chemistry, Articles 203 (1), 31−36.

Juncos, C., 2002. Etudes des phénomènes migratoires du ^{90}Sr dans les sols naturels expérimentalement contaminés: Rapport DESS Chimie de l'Environnement et Développement Durable. Chambéry, University of Savoie.

Khaleel, R., Freeman, E.J., 1995. Variability and scaling of hydraulic properties for 200 area soils, Hanford site. WHC-EP-0883, US DOE Contract DE-ACO6-87RL10930.

Kirchner, G., Baumgartner, D., 1992. Migration rates of radionuclides deposited after the Chernobyl accident in various north German soils. The Analyst 117, 475−479.

Lefèvre, R., Sardin, M., Schweich, D., 1993. Migration of strontium in clayey and calcareous sandy soil: precipitation and ion exchange. Journal of Contamination Hydrology 13, 215−226.

Lefèvre, F., Sardin, M., Vitorge, J., December 1996. Migration of ^{45}Ca and ^{90}Sr in a clayey and calcareous sand: calculation of distribution coefficients by ion exchange theory and validation by column experiments. International Journal of Rock Mechanics and Mining Sciences and Geomechanics 33 (8), 351A−351A(1).

Marimon, M.M., 2002. On the sorption and diffusion of radionuclides on bentonite clay. PhD thesis. Stockholm: Royal Institute of Technology, Sweden. http://www.lib.kth.se/Sammanfattningar/marimon020902.pdf.

Maubert, H., Grauby, A., Ponzetto, V., 1988. Comparing predictions of two radioecological models with measured values. In: Desmet, G. (Ed.), Reliability of Radioactive Transfer Models. Elsevier Applied Science, London, pp. 114−126, 355 pp.

Mualem, Y., 1972. A new model for predicting the hydraulic conductivity of unsaturated porous media. Water Resources Research 12 (3), 513−522.

NSPCG User's Guide. http://rene.ma.utexas.edu/CNA/NSPCG/manuals/usernsp/, 1988.

Porflow User's Manual. http://www.acricfd.com/download/papers/PORFLOW.pdf, 2002.

Ranganathan, V., 1993. The maintenance of high salt concentrations in interstitial waters above the New Albany shale of the Illinois Basin. Water Resources Research 29 (11), 3659−3670.

Romano, C.G., Frind, E.O., Rudolph, D.L., 1999. Significance of unsaturated flow and seepage faces in the simulation of steady-state subsurface flow. Ground Water 37 (4), 625−631.

Simunek, J.T., Vogel, T., Van Genuchten, M.Th., 1996. Hydrus-2D, Simulating Water Flow and Solute Transport in Two Dimensional Variability Saturated Media. Version 1.0. US Salinity Laboratory USDA/ARS, Riverside, CA and IGWMC-TPS 53. Golden, Colorado School of Mines.

Serne, R.J., Le Gore V.L., 1996. Strontium-90 adsorption-desorption properties and sediment characterization at the 100 N-area. PNL-10899, Pacific Northwest National Laboratory, Richland, Washington.

Taylor, A.W., 1968. Strontium retention in acid soils of the North Carolina Coastal Plain. Soil Science 106, 440−447.

Tormos, J., Jouve, A., Revy, D., Millan-Gomez, R., Zanon, R., Erario, M.J., 1995. A rapid method for determining ^{90}Sr in contaminated samples of soil and plant. Journal of Environmental Radioactivity 27 (3), 193−206.

Van Genuchten, M.Th., 1980. A closed-form equation for predicting the hydraulic conductivity of unsaturated soils. Soil Science Society of America Journal 44, 892−898.

Walton, J.C., Otis, M.D., 1990. Concrete barrier performance in radioactive disposal in the unsaturated zone. Materials Research Society 176, 711−717.

Wang, X., Du, J., Tao, Z., Fan, Z., 2003. Migration characteristics of radionuclides $^{85+89}$Sr^{2+}, ^{134}Cs^{+}, ^{125}I^{-}, ^{75}SeO$_3^{2-}$ and $^{152+154}$Eu(III) in Chinese soils. Journal of Radioanalytical and Nuclear Chemistry 258 (1), 133−138.

Weng, G.P., Coudrain, A., Bendjoudi, H., Giraud, F., 2001. Modélisation du fonctionnement de la zone humide alluviale. Fonctionnement des zones humides riveraines du cours moyen des rivières, pp. 67−77. http://www.sisyphe.jussieu.fr/Internet/prnzh/fichiers/fullfile14.pdf.

Wiklander, L., 1964. Uptake, adsorption and leaching of radiostrontium in a lysimeter experiment. Soil Science 97, 168−172.

Wösten, J.H.M., Lilly, A., Nemes, A., Le Bas, C., 1999. Development and use of a data base of hydraulic properties of European soils. Geoderma 90, 169−185.

Xiongxin, D., Zuyi, T., 1999. Effect of carbonates on sorption and migration of radiostrontium in calcareous soil. Journal of Radioanalytical and Nuclear Chemistry 242 (3), 727−730.